Observation of exciton states in silver halide nanoparticles by cryo-electron spectroscopic imaging and electron energy-loss spectroscopy

Vladimir P. Oleshko,[a,b] **Sergei B. Brichkin,**[c] **Renaat H. Gijbels,**[a] **Willem A. Jacob**[d] **and Vladimir F. Razumov**[*c]

[a] Department of Chemistry, University of Antwerp (UIA), B-2610 Wilrijk-Antwerpen, Belgium. Fax: +32 3 820 2364
[b] Photochemistry Centre, N. N. Semenov Institute of Chemical Physics, Russian Academy of Sciences, 117421 Moscow, Russian Federation. Fax: +7 095 936 1255
[c] Institute of Chemical Physics in Chernogolovka, Russian Academy of Sciences, 142432 Chernogolovka, Moscow Region, Russian Federation. Fax: +7 095 515 3588
[d] Department of Medicine, University of Antwerp (UIA), B-2610 Wilrijk-Antwerpen, Belgium. Fax: +32 3 820 2603

Electron excitations in Ag(Br,I) nanocrystals (attributed to excitons and plasmons possibly superimposed on interband transitions) and many-electron effects have been observed for the first time by cryo-electron spectroscopic imaging and electron energy-loss spectroscopy.

Small AgX (X=Cl, Br, I) particles exhibit remarkable transformations of optical and photochemical properties due to size confinement effects.[1,2] Analytical electron microscopy (AEM) allows the combination of a variety of signals and contrasting effects caused by inelastic scattering. The use of electron energy-loss spectroscopy (EELS) and electron spectroscopic imaging (ESI) can provide new insights into the crystalline and electronic structures of AgX particles. However, limitations arising from the insulating properties and beam sensitivity of AgX hamper AEM utilisation. Therefore, the potentials of cryo-AEM techniques in the case of such labile species should be estimated. To our knowledge, this paper presents the first application of cryo-ESI/EELS in which electron energy losses in $AgBr_{0.95}I_{0.05}$ nanocrystals synthesised by a double jet method at pBr = 3.5 and T = 35 °C, are studied.

Experimental details on specimen preparations and ESI/EELS analyses have been described elsewhere.[3,4] The electron energy-loss spectrum and a series of images of truncated cubic nanocrystals deposited on an amorphous carbon film *ca.* 20 nm in thickness at different energy losses are shown in Figure 1. The electron intensity changes due to the background decay, intersecting with the low-loss fine structure (5–16 eV), with the volume plasmon (*ca.* 23 eV) and with minor inner-shell bands (55–70 eV). This leads to contrast reversals. By tuning the energy loss, this allows the visualisation of excitations concerned with certain electron energy losses.[4] The coherent contribution of elastically scattered electrons to the contrast was separated in the zero-loss mode (0±5 eV) from the partially coherent contribution of inelastically scattered electrons. This avoids blurring of the images due to chromatic aberration which is the case in conventional transmission mode (CTEM). Filtering up to 100 eV showed that the Bragg contrast of disperse AgX matter is also preserved in inelastic scattering processes.

Even blurring of images by aberrations due to the angular distribution of inelastic scattering was found to be insignificant in this range.

In the first stage of a cascade of electron–solid interactions, electrons hit the crystal causing an internal ionisation with accompanying generation of excitons. Selection of exciton losses at $E = 16 \pm 5$ eV resulted in a weak rim around the crystals extending for distances of a few nanometers away from the particle (see Figure 1 and an enlarged micrograph in Figure 2), which corresponds satisfactorily to the expected exciton radius of 2.5 nm for AgX (X = I, Br).[2] Probably, swift electrons do not strike the particle directly but cause a polarisation inside it. When positioning the energy window at the volume loss ($E = 25 \pm 5$ eV), a bright excitation was created inside the support, since the latter contributes to the peak at 23 eV. Next the windows were placed at $E = 50 \pm 5$, 75 ± 5 and 100 ± 5 eV. This resulted in a complete contrast reversal due to the background decay, as shown in Figure 1. This allowed excitations in the crystals caused by plasmons possibly superimposed with some contribution of core 4p (Ag^+) and 3d (Br^-) excitations to be visualised.[4] The excitation probability decreased exponentially with distance from the particle surface. At 50 and 75 eV the fringes around the particles were easily distinguished at distances of 10–20 nm (see Figure 1 and an enlarged micrograph in Figure 2). The non-uniform contrast and darker areas inside the crystals were referred to predominant surface excitations (particularly near the edges). As was pointed out by Batson,[5] when the fields due to surface plasmons reach throughout the structure, they couple and the probability of their being generated becomes periodic in the size of the system. Since electronic sum rules must be satisfied,[5,6] the presence of surface excitations necessarily reduces the strength of the bulk plasmon excitations. As a result, the volume plasmons should exhibit similar periodic behaviour. Coupling of surface and volume losses could then cause an oscillation of their intensities with increasing particle size.

The low loss range is dominated by collective outer shell excitations superimposed with interband transitions and by excitations from defect levels into unoccupied states.[6,7] These scattering processes are sensitive to changes in density of states in both conduction and valence bands. The shape of the spectra of supported particles is influenced by excitations in the support, particle packing density and morphology. In order to minimise interference of AgX and support, particles were deposited on holey carbon films. Figure 3(*a*)–(*c*) shows a series of low-loss and inner-shell EEL spectra. Removal of plural scattering effects (curve *2*) by the use of a Fourier-log deconvolution[7] enabled an improvement in the spectral resolution. The single-scattering intensity for low losses expressed as the differential energy-loss probability dp/dE is related to the imaginary part of the reciprocal of the complex permittivity $\varepsilon(\vec{q},E)$ as a function of wave vector $\vec{q}$ and energy E. This reflects the local dielectric response of the media:[6,7]

$$\frac{dp}{dE} \propto \text{Im}\left[-\frac{1}{\varepsilon(\vec{q},E)}\right]\ln\left(1 + \frac{\beta^2}{\theta_E^2}\right),$$

where β is the collecting semiangle and θ_E is the characteristic scattering angle. The second term takes into account the angular dependence of the energy-loss probability, which affects the resolution of energy-loss spectra and allows various additional data to be obtained (angularly resolved EELS, Compton scattering). The permittivity is defined as $\varepsilon(\vec{q},E) = \varepsilon_1(\vec{q},E) + i\varepsilon_2(\vec{q},E)$, where the real part $\varepsilon_1(\vec{q},E)$ describes the specimen polarisability, while the imaginary part $\varepsilon_2(\vec{q},E)$ is related to specimen absorption. For energy losses $E \leq \hbar\omega_p = \hbar[ne^2/(\varepsilon_0 m)]^{1/2} = 21.4$ eV, the energy-loss function $\text{Im}\{-1/[\varepsilon(\vec{q},E)]\}$ describes collective excitations of outer shell electrons against the ionic background. Here ω_p is the resonance frequency of plasma oscillations, n is the electron density, e is the electron charge, ε_0 is the vacuum permittivity

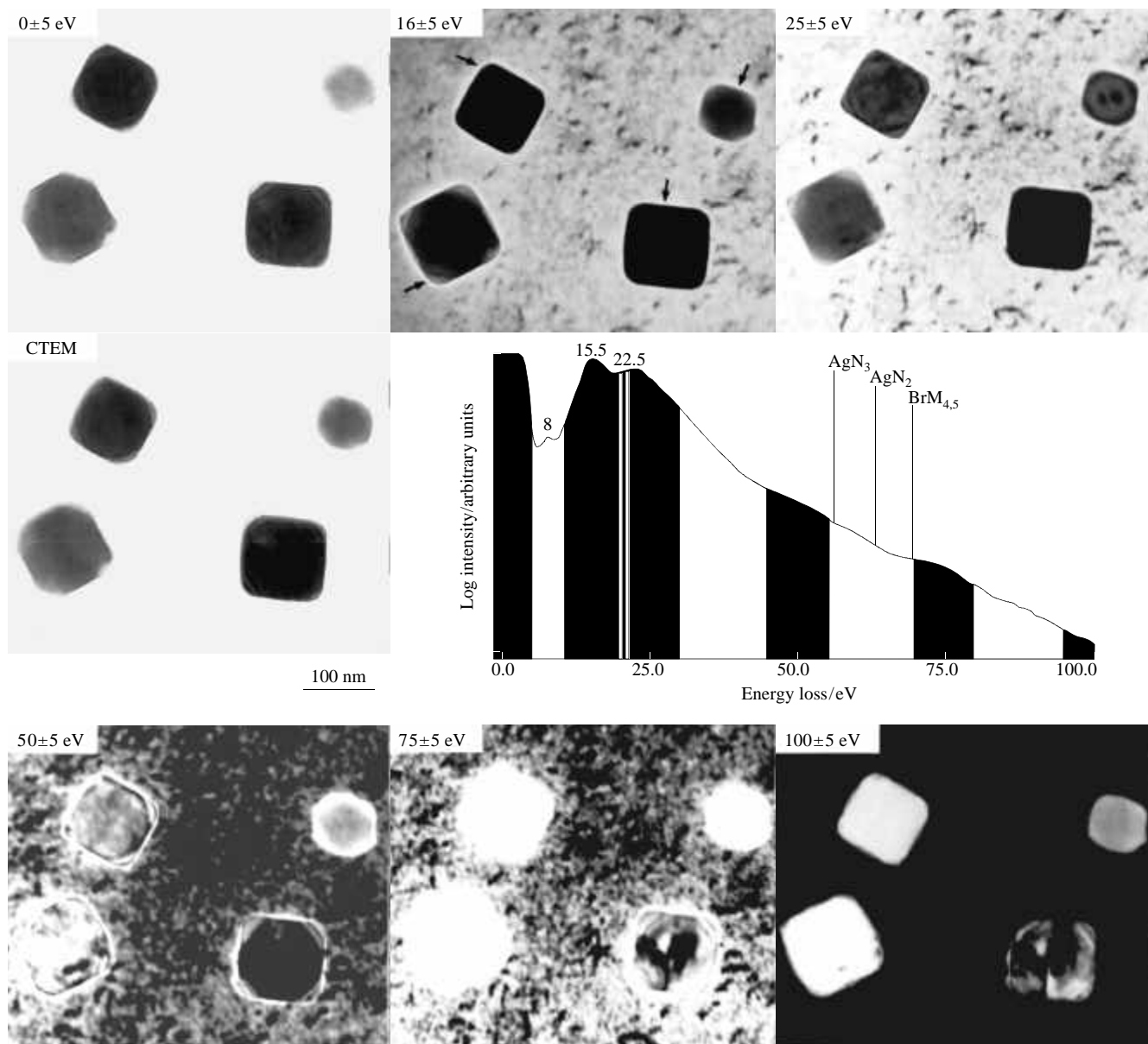**Figure 1** Low-loss spectrum and images of Ag(Br,I) nanocrystals at different energy losses in the range 0–100 eV, 10 eV window, $T = -177$ °C. Arrows indicate rims around the crystals at $E = 16\pm5$ eV assigned to excitons.

and m is the electron mass. The value was calculated taking into account valence 4d (Ag^+) and 4p (Br^-) electrons in a first approximation as quasi-free. Even with $m = m_0$, this is close to
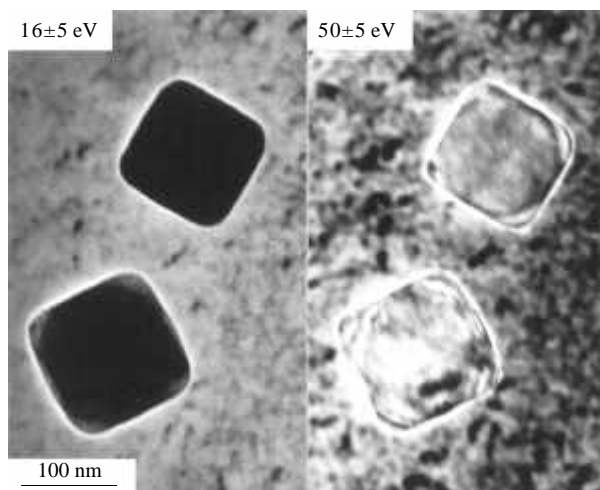

Figure 2 Enlarged energy-filtered images of Ag(Br,I) nanocrystals at 16 ± 5 and 50 ± 5 eV with fringes outside of the particles.

the experimental value within the accuracy of measurements. The function $\text{Im}\{-1/[\varepsilon(\bar{q},E)]\} = \varepsilon_2/(\varepsilon_1^2 + \varepsilon_2^2)$ has a peak corresponding to certain oscillations, when ε_1 is zero or at least has a local minimum (this points out the instability of the electron system towards small external perturbations) and ε_2 is still small enough (this indicates minimal damping of oscillations due to absorption). So, the volume plasmon at $E_p = 22.5$ eV reflects the correlated motion of the valence 4d electrons affected by the band structure. Although the energy of surface plasmons, E_s, is often described as approximately $E_s = E_p/\sqrt{2}$,[6,7] it is arguable whether the peak at 15.5 eV can be considered as a surface and/or defect plasmon, in view of its relatively high intensity. Moreover, quasi free electrons taking part in these excitations are present in metals, but not in insulating AgX crystals. Polarisation waves formed by weakly bound electron–hole pairs (Mott–Wannier excitons) are a prominent type of excitation for AgBr.[8] Iodine in AgBr acts as an isoelectronic trap for holes producing a positively charged centre, which can subsequently neutralise itself by binding an electron, thus forming a bound exciton.[9] Interband transitions caused by mixing of the Ag 4d states with the halogen 4p states at various points in the Brillouin zone[8] may also occur. In accordance with the assignment of the UV absorption and reflectivity spectra of AgBr,[8,10] the feature at 5 eV was
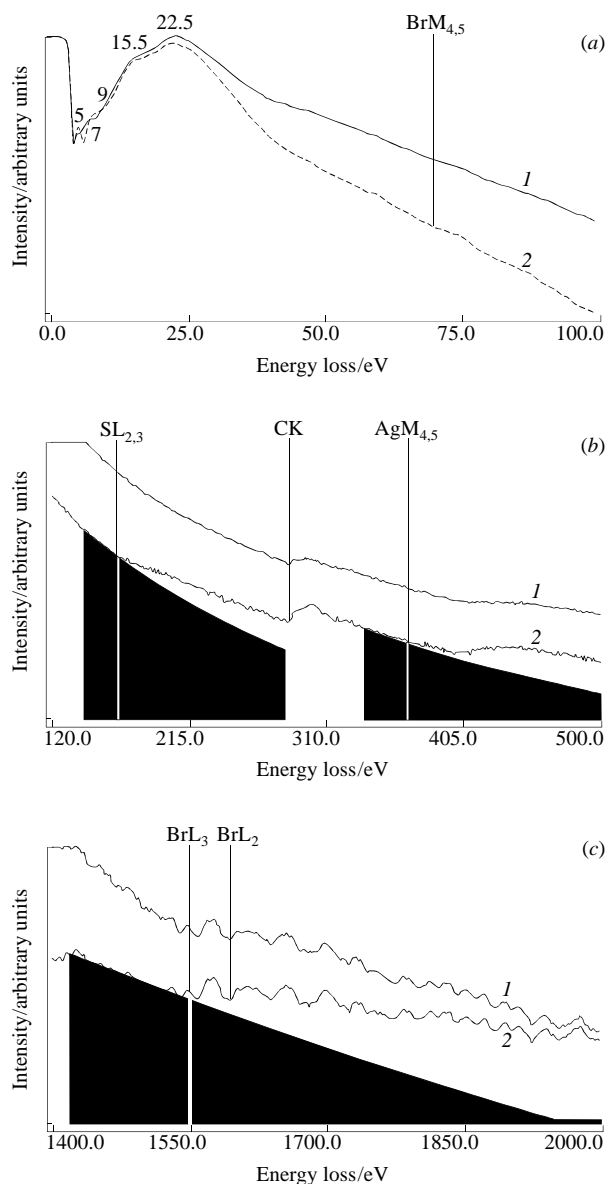
Figure 3 EEL spectra of Ag(Br,I) nanoparticles at $T = -177$ °C: (*a*) the low-loss region, an experimental spectrum (curve *1*) and a single scattering distribution (curve *2*); (*b*) the inner shell excitation region; (*c*) the smoothed $BrL_{2,3}$ edge.

attributed to unresolved direct exciton transitions involving the spin–orbit split valence and the conduction band states at point Γ, *i.e.* (Γ_8^-, $\Gamma_6^- \to \Gamma_6^+$). The states at *ca.* 7 eV probably belong to proposed exciton transitions at point X [unresolved (X_6^-, X_6^-, X_7^-) $\to X_6^+$],[10] possibly superimposed with interband transitions. The peak at 15.5 eV energy loss may be referred to exciton transitions particularly with $L_{4,5}^-$ and Γ_6^+ symmetries and/or to higher exciton states formed at points different from Γ and L in the Brillouin zone as well.

References

1 K. P. Johansson, A. P. Marchetti and G. L. McLendon, *J. Phys. Chem.*, 1992, **96**, 2873.
2 A. P. Marchetty, K. P. Johansson and G. L. McLendon, *Phys. Rev. B.*, 1993, **47**, 4268.
3 V. P. Oleshko, R. H. Gijbels, W. A. Jacob and M. V. Alfimov, *Microbeam Analysis*, 1995, **4**, 1.
4 V. P. Oleshko, R. H. Gijbels and W. A. Jacob, *J. Microscopy*, 1996, **183**, 27.
5 P. E. Batson, *Surf. Sci.*, 1985, **156**, 720.
6 L. Reimer, *Energy-Filtering Transmission Electron Microscopy,* in *Springer Series in Optical Sciences*, ed. L. Reimer, Springer–Verlag, Berlin, 1995, vol. 71, pp. 1, 151, 347.
7 R. F. Egerton, *Electron Energy-Loss Spectroscopy in the Electron Microscope*, 2nd edn., Plenum Press, New York, 1996, pp. 131, 433.
8 N. J. Carrera and F. C. Brown, *Phys. Rev.*, 1971, **B4**, 3651.
9 W. Czaja and A. Baldereschi, *J. Phys. C: Solid State Phys.*, 1979, **12**, 405.
10 F. Bassani, R. S. Knox and W. B. Fowler, *Phys. Rev.*, 1965, **A4**, 1217.